Estimation of Slip Angles using a Model Based Estimator and GPS

Rusty Anderson* and David M. Bevly**

Abstract— **This paper demonstrates a method for estimating key vehicle states and sensor biases using Global Positioning System (GPS) and an Internal Navigation System (INS). Two Kalman filters, a model based filter and a Kinematic filter, are used to integrate the INS sensors with GPS heading and velocity to provide a high update rate of the vehicle states and sensor biases. Additional key vehicle parameters, such as tire-cornering stiffness, are identified and used to correct the model based estimator. The vehicle estimated states compare favorable with values predicted with a theoretical model**

I. INTRODUCTION

A critical component of many vehicle control systems such as stability control and lateral control systems is the accurate knowledge of vehicle sideslip and yaw rate [1, 2]. Yaw rate can be measured with a low-cost rate gyroscope. However, sideslip measurements require expensive speed over ground sensors. Recently, it has been shown that sideslip can be directly measured with a two-antenna GPS attitude system [3]. This method, though less expensive than the speed over ground sensor, only provides measurements in the 10-20 Hz range and are not available when there is a poor visibility of the sky .

Since sideslip measurement is not available on production cars, this key state has to be estimated. A common practice is to estimate sideslip by integrating inertial sensors [4]. This method can lead to inaccurate estimates of sideslip due to vehicle roll, road bank, or noise and bias on the sensor. Another method of estimating sideslip is through a non-linear observer with a yaw rate measurement [5]. However, sideslip is unobservable with a yaw rate and steer angle measurement when the vehicle is reaching neutral steer characteristics. It has been shown that sideslip can be estimated by comparing an integrated gyro to GPS velocity heading information using a Kinematic Kalman filter to account for these errors [6, 7]. While this estimator is able to account for bias in the sensor it is unable to account for scale factor errors. If there is a scale factor error in the gyro, the estimation of sideslip will grow during turning. Additionally, while this method can provide an accurate estimate of sideslip it does not give any indication that the model used by the controller is correct.

Sideslip can also be estimated with a model based Kalman filter using measurements of steer angle and yaw rate [8]. However, this requires that the vehicle parameters be correctly identified in order to accurately estimate sideslip. This can be difficult because key parameters, such as tire cornering stiffness and weight split, can vary over time. However, it has been shown that GPS based sideslip estimates can be used to estimate tire cornering stiffness [7]. This paper explores a model based Kalman filter with GPS velocity measurements to estimate sideslip, heading, and yaw rate.

II. BICYCLE MODEL AND EQUATIONS OF MOTION

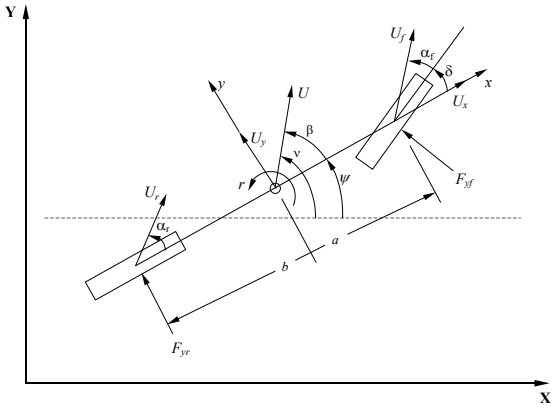

Figure 1. Bicycle Model

Figure 1 is a schematic of the bicycle model of a vehicle. As seen in the figure the sideslip (β) is the difference of heading (ψ) and course angle (v) of the vehicle [9]. The equations that describe the lateral dynamics of the bicycle model can be found by summing the forces and moments about the center of gravity as shown in Equation (1).

* Currently a Graduate Student at Auburn University department of Mechanical engineering, Auburn Al 36849 (anderru@auburn.edu)

** Assistant Professor Department of Mechanical Engineering

$$\sum F_y = F_{yf} + F_{ye} = M(\dot{U}_y + Ur) - mg\sin(\theta_{bank})$$
$$\sum M_y = aF_{yf} - bF_{yr} = I_z \quad (1)$$
$$F_{yf} = C_{\alpha f}\alpha_f \approx C_{\alpha f}\left(\beta + \frac{ar}{U} - \delta\right)$$
$$F_{yr} = C_{\alpha f}\alpha_r \approx C_{ar}\left(\beta - \frac{br}{U}\right)$$

Note that the tire forces include the lateral handling forces and the effect of road bank. Road bank can be accounted for either by using GPS position measurements in conjunction with knowledge of the highway infrastructure or by estimating the bank angle [10]. Figure 2 is an experimental plot of the understeer of a Chevrolet Blazer (with a wheel base length of 2.591m) on an eight degree banked fixed radius turn (of 145 m). The .5 degree decrease in steer angle, due to effects of road bank angle as shown in Equation (1) can be seen in Figure 2.

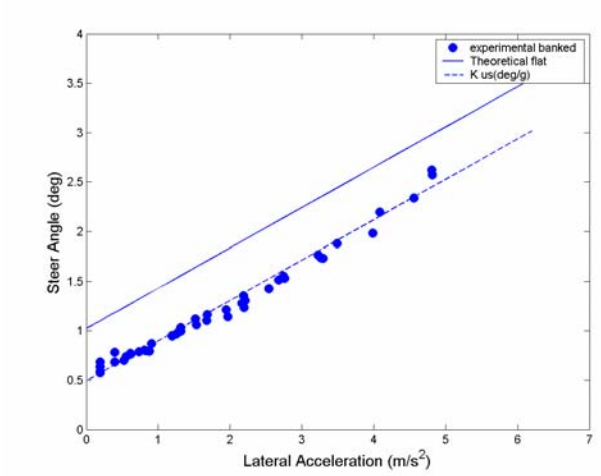

Figure 2 Steady State Cornering on banked turn (k_us = 4 deg/g)

III. KALMAN FILTERS

The GPS measurements are integrated with the yaw rate through two types of estimators, a Kinematic Kalman filter and a model based Filter. The Kalman filter is comprised of a measurement update, which is only performed when the measurements are available, and a time update [9], which is updated at each time step. The measurement update is described by Equation (2).

$$L_k = P_k * Cd^T * (Cd * P_k * Cd^T + R_v)^{-1}$$
$$X_k = X_k + L_k(y_{meas} - Cd * x_k) \quad (2)$$
$$P_k = (I - L_k * Cd)P_k$$

Where L= Kalman gains

P= State Error covariance matrix

C= observation matrix describing the available measurement

R=measurement noise covariance matrix

X=state estimate

The time update, which is the propagation of the state in time, can be seen in Equation (3).

$$\hat{x}_{k+1} = Ad * x_k + Bd * u_k \quad (3)$$
$$P_{k+1} = Ad * P_k * Ad^T + Q_d$$

where Ad= the discrete A matrix

u= input

Q_d = the discrete process noise covariance matrix

$$\approx BQ_cBT_s$$

Q_c= the continuous process noise covariance matrix

An estimator based only on the Kinematic relationships between heading and yaw rate is called the Kinematic Kalman Filter (KKF). The state space form for the Kinematic Kalman filter is shown in Equation (4).

$$\begin{bmatrix} \dot{\psi} \\ \dot{b}_{gyro} \end{bmatrix} = \begin{bmatrix} 0 & -1 \\ 0 & 0 \end{bmatrix}\begin{bmatrix} \psi \\ b_{gyro} \end{bmatrix} + \begin{bmatrix} 1 \\ 0 \end{bmatrix} r \quad (4)$$

$$C = \begin{bmatrix} 1 & 0 \end{bmatrix}\begin{bmatrix} \psi \\ b_{gyro} \end{bmatrix} \qquad Q_d = T_s^2 I \begin{bmatrix} \sigma^2_{gyro} & 0 \\ 0 & \sigma^2_{bias} \end{bmatrix} I$$

$$C = \begin{bmatrix} 0 & 0 \end{bmatrix}\begin{bmatrix} \psi \\ b_{gyro} \end{bmatrix} \qquad R_d = \begin{bmatrix} \sigma^2_{v_{gps}} & 0 \\ 0 & \sigma^2_{bias} \end{bmatrix}$$

The two states estimated are the heading of the vehicle and the bias on the yaw gyro. The input into the system is yaw rate from the gyroscope. During straight driving the gyro bias is estimated using the GPS heading (ν). The observation matrix is set to zero during turning which turns off the bias estimate and integrates the gyro, with the estimated bias removed. An estimate of sideslip is obtained during turning by comparing the GPS course angle with the integrated gyro heading.

The second estimator used in this paper is a model-based estimator. The estimator's state space form comes from linearizing the bicycle model dynamics equations given in Equation (1). The state space equations for the estimator can be seen in Equation (5).

$$\begin{bmatrix} \dot{\beta} \\ \dot{r} \\ \dot{\psi} \\ \dot{b}_{gyro} \end{bmatrix} = \begin{bmatrix} \frac{-C_{af} - C_{ar}}{mV} & \frac{-aC_{af} + bC_{ar}}{mV^2} - 1 & 0 & 0 \\ \frac{-aC_{af} + bC_{ar}}{I_z} & \frac{a^2C_{af} + b^2C_{ar}}{I_z * V} & 0 & 0 \\ 0 & 1 & 0 & 0 \\ 0 & 0 & 0 & 0 \end{bmatrix}\begin{bmatrix} \beta \\ r \\ \psi \\ b_{gyro} \end{bmatrix} + \begin{bmatrix} \frac{C_{af}}{m * V} \\ \frac{aC_{af}}{I_z} \\ 0 \\ 0 \end{bmatrix}\delta \quad (5)$$

$$C = \begin{bmatrix} 0 & 1 & 0 & 1 \\ 1 & 0 & 1 & 0 \end{bmatrix}\begin{bmatrix} \beta \\ r \\ \psi \\ b_{gyro} \end{bmatrix} \qquad Q_d = B_w \begin{bmatrix} \sigma^2_\delta & 0 \\ 0 & \sigma^2_{bias} \end{bmatrix} B_x^T Ts$$

$$R_d = \begin{bmatrix} \sigma^2_r & 0 \\ 0 & \sigma^2_\psi \end{bmatrix}$$

GPS velocity provides a measurement of vehicle course

(ν) which is sideslip plus heading as shown if Figure 1. The states being estimated by Equation (5) are sideslip (β), yaw rate (r), heading (ψ), and gyro bias (b_{gyro}). Note that this system is observable even if the vehicle is neutral steer. Additionally, sideslip, yaw rate, and heading are observable with only the GPS measurement, which provides system redundancy. It will be shown in the following sections that this estimator can provide a cleaner estimate of the needed states and provides better estimate of sideslip in the presence of a gyro scale factor error**.** This model based estimator also provides some insight into determining the model accuracy.

The Kalman filter also provides a covariance of how well the state is being estimated called the state error covariance matrix, P. Table I shows the gyroscope and GPS course measurements noise (at 30 m/s) for various sample rates and the corresponding predicted state estimation error which are form the state error covariance matrix using the model based estimator. Note that the predicted state estimation error for the model based estimator assumes a perfect state estimator model and known process noise covariance matrix. The measurement noise is assumed to increase with the square root of the bandwidth (or sample rate). Although most GPS receivers have slow output rates, some output data as fast as 50 Hz and it is possible to get the measurements at even higher update rates.

TABLE I
STATE ESTIMATION ERROR AT VARIOUS SAMPLE RATES(AT V= 30 M/S)

	$\sigma_{\hat{\beta}}$ deg	$\sigma_{\hat{r}}$ deg/s	σ_r deg/s	σ_ν deg
5 Hz	.0348	.0636	0.0671	.0086
20 Hz	.0697	.1272	0.1342	.0171
50 Hz	.1101	.2012	0.2121	.0270
100 Hz	.1558	.2845	0.3	.0382

Figure 2 is the graph of the error covariance matrix for the estimation of sideslip using both the model based estimator and the Kinematic Kalman filter during two 180° turns on a test track. The Kinematic Kalman filter provides an estimate of the state covariance error of heading. The error of sideslip if formed in Equation (6).

$$\sigma_{\hat{\beta}} = \sqrt{\sigma_{\psi}^2 + \sigma_{v_{GPS}}^2} \qquad (6)$$

$$Where \quad \sigma_{v_{GPs}} = \frac{\sigma_{U_{GPS}}}{U} \approx \frac{.05}{U}$$

Therefore, the estimate of the sideslip is more accurate at higher velocities as seen in Figure 2. The growth in the error covariance for the Kinematic Kalman filter is due to the fact the estimator is turned off during the turning maneuvers. Note that the error is only due to the modeled stochastic error in the Kinematic Kalman filter and does not include errors such as gyro scale factor error.

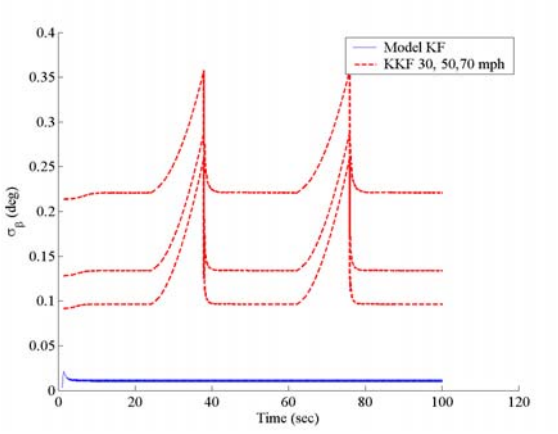

Figure 3 State Error Covariance

Figure 3 also shows that the model based estimator can provide a much more accurate estimate of the sideslip angle (assuming the estimator has the correct model parameters).

The process noise matrix on the model based estimator is a measure of the plant disturbance and sometimes used as a measure of plant uncertainty. Figure 4 shows how the accuracy of the sideslip estimate varies with increasing process noise on the steer angle input.

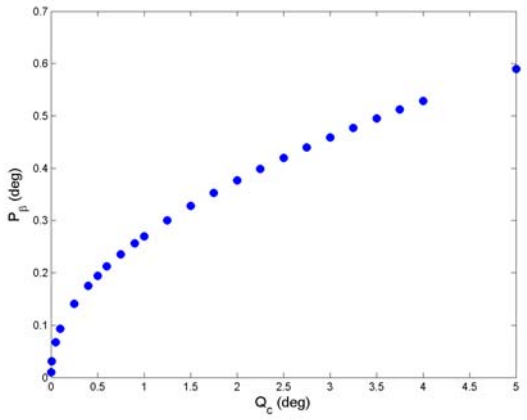

Figure 4 Process Noise Vs Error

IV. SIMULATED RESULTS

A simulation was performed in order to compare the effects of incorrect model parameters with a yaw rate scale factor error present on both the model based and Kinematic Kalman filter. The simulation used parameters of a Chevrolet Blazer driving around two 180° constant radius turn with process and sensor noise. A 2% scale factor error, which is within the normal gyro specification, was added to the gyro measurement during simulation. First, a Kinematic Kalman filter was used to estimate the sideslip of a vehicle and the results of which are given in Figure 5. This figure shows that the presence of a small scale factor

error can lead to large error in the sideslip angle estimation.

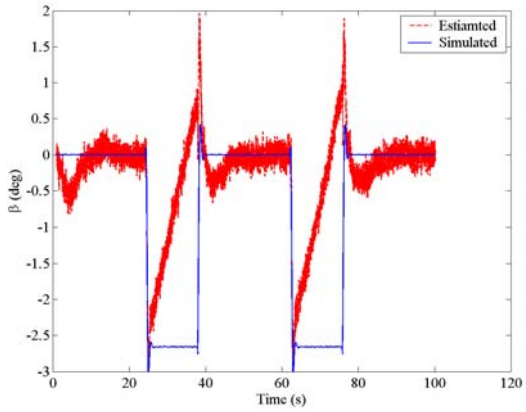

Figure 5 KKF estimation

Next the model based estimator was used with the parameters of a different vehicle (i.e. incorrect weight, weight split, mass moment of inertia, and tire cornering stiffness). Figure 6 shows the simulated and estimated sideslip and yaw rate and reveals how model parameter error leads to biased estimations of the states.

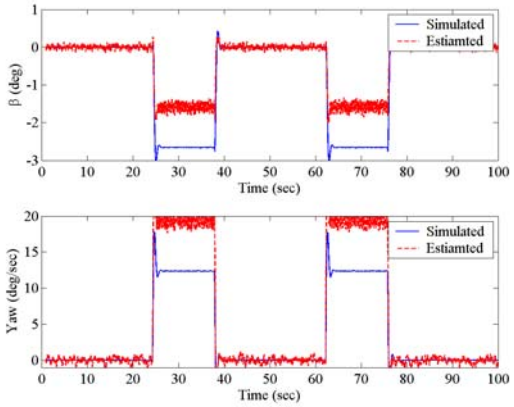

Figure 6 Incorrect model estimation

The simulation was repeated again using the Blazer, where the estimator was given the correct vehicle parameters. The results of the estimation of sideslip and yaw rate are shown in Figure 7.

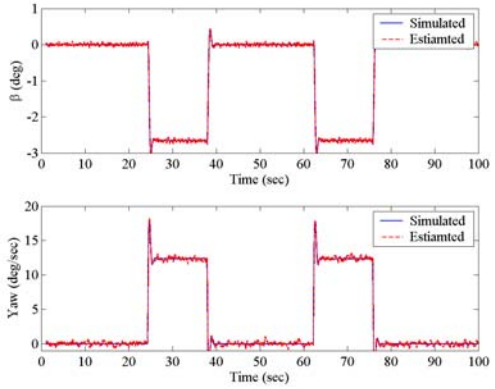

Figure 7 Correct model estimation

Figure 7 demonstrates that with the correct parameters the estimation of sideslip and yaw rate is very accurate even in the presence of a scale factor error.

From Figure 6 and 7 it can be seen that yaw rate and sideslip reach steady state values relatively quickly during heavy turning. By manipulating Equation (1), the equations for steady state yaw rate and steady state sideslip can be derived and are given in Equation (7). Steady state yaw rate and sideslip are dominated by the weight split and the tire cornering stiffness. Therefore for a steer input that is below the bandwidth of the vehicle's yaw dynamics, which is almost all driver inputs, the yaw rate and sideslip estimation accuracy is dominated by the vehicles weight split and tire cornering stiffness.

$$r_{ss} = \frac{V}{L + V^2 K_{us}}\delta$$
$$\beta_{ss} = \frac{br}{V} - \frac{m_r V r}{C_{\alpha f}} \qquad (7)$$
$$where \quad K_{us} = \frac{W_f}{C_{\alpha f}} - \frac{W_r}{C_{\alpha r}}$$

V. Experimental Results

A 2000 Chevrolet Blazer (with known vehicle parameters) was instrumented for testing the model based Kalman filter. The Blazer was equipped with a string potentiometer, from Space Age Controls, that measures steer angle at the wheel and is sampled at a rate of 100Hz. The Blazer was also instrumented with a 6 axis Bosch IMU, consisting of 3 accelerometers and 3 rate gyros, which was also sampled at a rate of 100Hz. In addition, the Blazer was instrumented with a Starfire GPS receiver, which provides 5 Hz GPS measurements.

First, an experimental run was taken in a parking lot doing extreme cornering maneuvers. The measurement update was updated at 5Hz to coincide with the GPS measurement. If GPS is not available the estimates are updated with only the gyro measurement. The sideslip and

yaw rate (actual and experimental) of the experiment can be seen in Figure 8. Note the value for the actual sideslip was calculated by comparing the GPS course angle to an integrated yaw rate with scale factor error and bias removed. The estimated value uses the raw yaw rate measurement with no compensation for biases or errors removed.

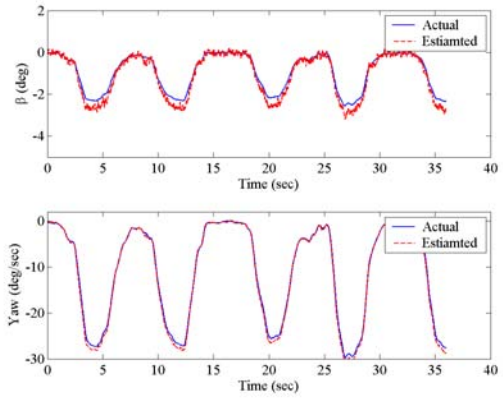

Figure 8 estimation of cornering test

Even though the parameters are not exactly precise, this still leads to a good estimate of sideslip with the presence of a scale factor error on the gyro.

The estimator also provides two residuals, which are the difference between the actual measured and the estimated measurement in Equation (2), which can be used to check the model accuracy. The residuals should be white noise with the following variances.

$$\sigma_{GPS\_residual} = \sqrt{\sigma_{\nu}^2 + \sigma_{\hat{\psi}}^2 + \sigma_{\hat{\beta}}^2} \qquad (8)$$

$$\sigma_{gyro\_residual} = \sqrt{\sigma_r^2 + \sigma_{\hat{r}}^2}$$

A GPS measurement is needed in order for the second residual, which can provide greater insight on the accuracy of the model. The graph of the residuals of the yaw rate and GPS heading is shown in Figure 9

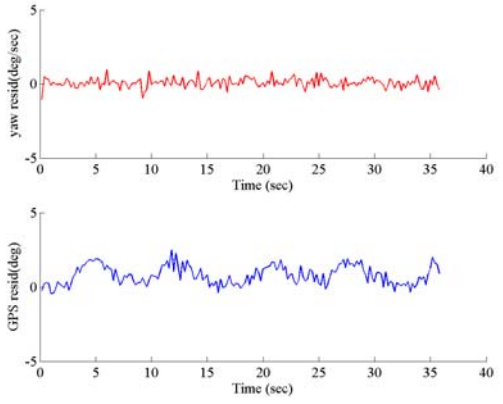

Figure 9 residuals of cornering test

Looking at the residuals it can be seen that there are incorrect parameters in the estimator because the residuals are not random white noise. It may be possible to estimate the parameters during a GPS measurement update in order minimize the residual errors.

Next data was collected from a 180 degree test track with an 8 degree bank turn. Again for the estimator, neither the scale factor error nor the bias was removed. The sideslip and yaw rate from this experiment can be seen in Figure 10.

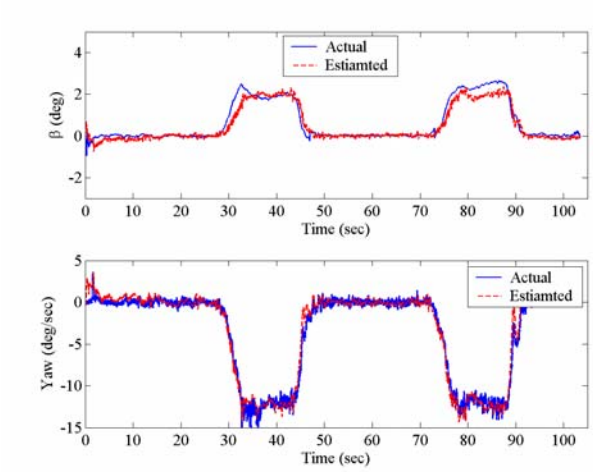

Figure 10 Estimation on banked turn

The error in the estimation of side slip is due to the presence of the banked turn. Recall that Figure 1 shows how the bank caused the steer angle to be slightly less that it would be on flat ground. This causes an incorrect steer angle measurement to be fed to the estimator. This error is still less than the error received if a lateral accelerometer was integrated [1]. Again examining the residuals provided by the estimator allows for a verification of model accuracy. The residuals for this experiment can be seen in Figure 11.

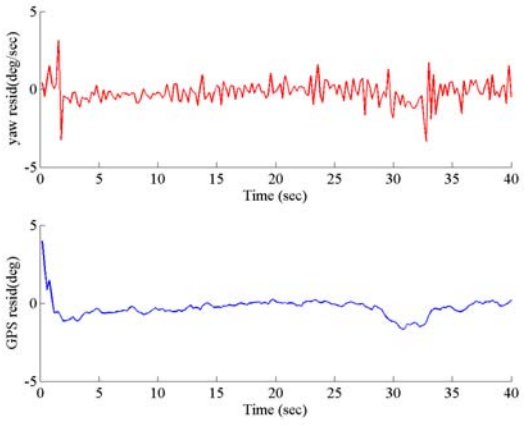

Figure 11 residuals of banked turn

It has been shown that tire cornering stiffness can be determined with the correct estimation of sideslip [7]. If this parameter can be updated and fed into the estimator, this would help provide a better model with which to estimate sideslip. A continuous estimation of tire cornering stiffness will compensate for errors in other parameters, such as incorrect weight split. If the scale factor error is known in advance or removed from the gyro, then a Kinematic Kalman filter can be used to estimate sideslip, which can then be used to estimate tire cornering stiffness to help correct the model. The results from using a Kinematic Kalman filter to update the parameters of the model based estimator on the high cornering experiment are shown in Figure 12

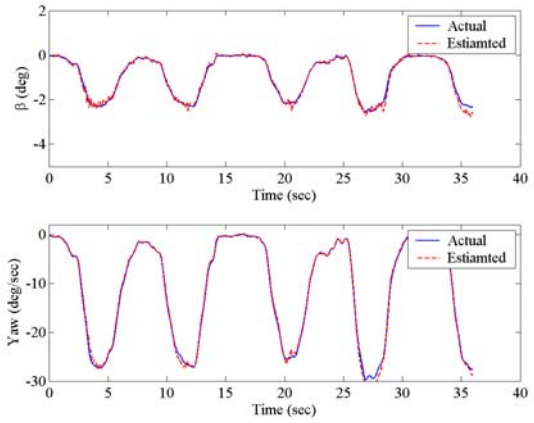

Figure 12 estimation of cornering test updating parameters

The residuals for this experiment are shown below in Figure 13. The indication that the residuals are close to white noise indicates that estimator is giving an accurate estimate of the states. The errors that remain are caused by some un-modeled vehicle dynamics.

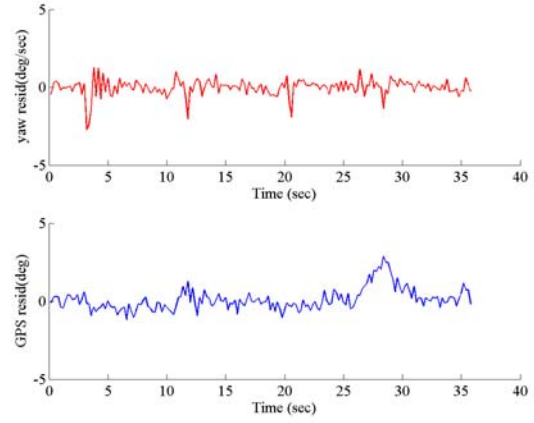

Figure 12 residuals of estimation when updating parameters

VI. Conclusion

This paper has shown that the model based estimator using GPS measurement along with the correct model parameters can correctly estimate sideslip, yaw rate and heading in the presence of gyro scale factor error and banked turns. By examining the residuals, provided by the estimator, model parameters can be updated with the measurement update, thus giving the controller a correct model. This has been shown with experimental data taken during extreme cornering maneuvers and on a fixed radius test track with an eight degree bank.

Future work involves nonlinear estimation in attempts to correctly estimate key vehicle parameters such as weight split and tire cornering stiffness. Also, examining performance of the estimator while the vehicle is operating in the handling limits.

VII. Acknowledgements

The author would like to thank Buzz Powell and the Nation Center for Asphalt Testing (NCAT) for the use of the test track.

VIII. References

[1] Nishio H., et. al., "Development of Vehicle Stability Control based on Vehicle sideslip angle Estimations," SAE paper No. 2001.

[2] Daily, R. Bevly, D.M. "The use of GPS for Vehicle stability control system" *IEEE transactions on Industrial Electronic, VOL. 51, No. 2, April 2004.*

[3] Ryu, J., Rossetter, E.J., Gerdes, J.C., "Vehicle sideslip and Roll parameters Estimation Using GPs," Proceeding of the AVAC 2000.

[4] Hac, A., and Simpson, M. "Estimation of Vehicle Sideslip Angle and Yaw Rate" SAE Paper Number 2000-01-0696.

[5] Kiencke U., Daiss, A., "Observation of Lateral Vehicle Dynamics." Proceedings of the 1996 IFAC, p7-10

[6] Bevly, D.M. et. al. "The Use of GPS Based Velocity Measurements for Improved Vehicle State Estimation." Proceeding from the ACC 2000, June 2000, Chicago, IL.

[7] Bevly .M. Sheridan, R., Gerdes, J.C. "Integrating INS sensors with GPS with GPS Velocity measurements for Continuous Estimation of Vehicle sideslip and Tire Cornering Stiffness" Proceedings from 2001 ACC

[8] Farrlly, J., Wellstead P., "Estimation of vehicle Lateral Velocity," Proceedings from the 1996 IEEE conference on Control Application

[9] Gillespie, Thomas D. 1992 *Fundamentals of vehicle Dynamics*. Warrendale Pa.

[10] Ryu, J., Gerdes, J.C., "Estimation of Vehicle Roll and Road Bank Angle. Proceedings from the ACC 2004, July 2004, Boston. MA.

[11] Stengel R., *Optimal Control and Estimation*, Dover ed. Dover Publications Meneola, New York, 1994.